the plant journal

SEB SOCIETY FOR EXPERIMENTAL BIOLOGY

The Plant Journal (2023) **116,** 416–431 doi: 10.1111/tpj.16381

Plant and fungal gene expression coupled with stable isotope labeling provide novel information on sulfur uptake and metabolism in orchid mycorrhizal protocorms

Silvia De Rose[1,†], Yukari Kuga[2,†], Fabiano Sillo[3], Valeria Fochi[1], Naoya Sakamoto[4], Jacopo Calevo[1,‡], Silvia Perotto[1,*] and Raffaella Balestrini[3,*]

[1]*Dipartimento di Scienze della Vita e Biologia dei Sistemi, Università degli Studi di Torino, Viale Mattioli, 25, 10125 Torino, Italy,*

[2]*Graduate School of Integrated Sciences for Life, Hiroshima University, Higashihiroshima, Hiroshima 739-8521, Japan,*

[3]*Consiglio Nazionale delle Ricerche, Istituto per la Protezione Sostenibile delle Piante, Strada delle Cacce 73, 10135 Torino, Italy, and*

[4]*Isotope Imaging Laboratory, Creative Research Institute, Hokkaido University, Sapporo 001-0021, Japan*

Received 22 February 2023; revised 27 June 2023; accepted 3 July 2023; published online 8 July 2023.
*For correspondence (e-mail raffaella.balestrini@ipsp.cnr.it; silvia.perotto@unito.it).
†These authors equally contributed to the work.
‡Present address: School of Molecular and Life Sciences, Curtin University, Perth, WA 6102, Australia

SUMMARY

Orchid mycorrhiza (OM) represents an unusual symbiosis between plants and fungi because in all orchid species carbon is provided to the host plant by the mycorrhizal fungus at least during the early stages of orchid development, named a protocorm. In addition to carbon, orchid mycorrhizal fungi provide the host plant with essential nutrients such as phosphorus and nitrogen. In mycorrhizal protocorms, nutrients transfer occurs in plant cells colonized by the intracellular fungal coils, or pelotons. Whereas the transfer of these vital nutrients to the orchid protocorm in the OM symbiosis has been already investigated, there is currently no information on the transfer of sulfur (S). Here, we used ultra-high spatial resolution secondary ion mass spectrometry (SIMS) as well as targeted gene expression studies and laser microdissection to decipher S metabolism and transfer in the model system formed by the Mediterranean orchid *Serapias vomeracea* and the mycorrhizal fungus *Tulasnella calospora*. We revealed that the fungal partner is actively involved in S supply to the host plant, and expression of plant and fungal genes involved in S uptake and metabolism, both in the symbiotic and asymbiotic partners, suggest that S transfer most likely occurs as reduced organic forms. Thus, this study provides original information about the regulation of S metabolism in OM protocorms, adding a piece of the puzzle on the nutritional framework in OM symbiosis.

Keywords: sulfur metabolism, orchid mycorrhiza, *Tulasnella*, *Serapias vomeracea*, gene expression, stable isotope tracer.

INTRODUCTION

Sulfur (S) is an essential macronutrient for all organisms, but conversion of inorganic to organic S compounds is primarily dependent on sulfate uptake and reduction in photosynthetic organisms and microorganisms (Takahashi et al., 2011). Sulfur is involved in multiple metabolic processes where it serves many functions as a structural constituent of amino acids (cysteine and methionine), coenzymes (S-adenosyl-methionine), prosthetic groups (iron–sulfur cluster), vitamins (biotin and thiamin), the antioxidant glutathione, sulfolipids, and secondary metabolites (Kopriva et al., 2019).

In green plants, S is the fourth most important nutrient element after nitrogen, phosphorus, and potassium, and S deficiency affects plant growth, plant performance, and yield (Hell, 1997; Zenda et al., 2021). For these reasons, S uptake and metabolism in plants have been extensively investigated (Kopriva et al., 2019; Li et al., 2020; Narayan et al., 2022).

Plants take up inorganic S from the soil mainly in the form of sulfate, which is then transferred to the shoot and reduced in the chloroplasts through the reductive sulfate assimilation pathway.

Uptake and internal transport of sulfate in plants, including translocation between different cell compartments, occurs

via sulfate transporters of the SULTR family (Li et al., 2020; Takahashi, 2019). SULTR is a multigene family of sulfate/H^+ co-transporters, and different categories of SULTR genes have been proposed according to their coding sequence homology, biochemical properties, and functions (Takahashi et al., 2011). In *Arabidopsis*, the two high-affinity sulfate transporters SULTR1.1 and SULTR1.2 are major players in sulfate absorption from the soil and are mainly located in root hairs and epidermal root cells (Takahashi et al., 2000), whereas the SULTR2.1 isoform seems responsible of translocation from roots to shoots. An additional role as a S sensor has been proposed for the SULTR1.2 transporter (Takahashi, 2019; Zheng et al., 2014). Inside the plant cells, transporters of the SULTR3 family may directly mediate sulfate import into the chloroplasts, where sulfate is reduced (Cao et al., 2013; Chen et al., 2019). Sulfate can be stored in the vacuole, and sulfate transporters of the SULTR 4 group seem to be responsible for sulfate efflux from this organelle under S deficiency (Takahashi, 2019; Takahashi et al., 2011).

Sulfur incorporation into biomolecules requires reduction of inorganic sulfate to sulfide. In plants, the reductive sulfate assimilation pathway starts with the ATP-dependent activation of sulfate to adenosine 5′-phosphosulfate (APS), followed by reduction to sulfite via an APS reductase, and then to sulfide. Condensation of sulfide with O-acetylserine (OAS) leads to the formation of the amino acid cysteine, which is either used directly in protein biosynthesis or for the synthesis of the amino acid methionine, of the redox control molecule glutathione, and of the methyl group donor S-adenosylmethionine (SAM). Starting from APS, the plant sulfate assimilation pathway bifurcates into two pathways: one is the reductive pathway described above, whereas the other involves an APS kinase and leads to the biosynthesis of 3′-phosphoadenosine 5′-phosphosulfate (PAPS), which serves as sulfate donor for sulfation of peptides, hormones, and secondary metabolites crucial for oxidative stress responses (Chan et al., 2019; Kopriva et al., 2012).

In nature, most plants form symbioses with mycorrhizal fungi that assist them with mineral nutrition (Balestrini & Lumini, 2018; Bucher et al., 2014; Genre et al., 2020). Different types of mycorrhizal fungi can be distinguished (arbuscular, ecto, ericoid, and orchid mycorrhizal fungi), depending on the morphology of their association with the host plant (Smith & Read, 2008).

Thanks to their extraradical mycelium, mycorrhizal fungi play a pivotal role in the acquisition of mineral nutrients because their hyphae can explore large volumes of soil and extend into soil micropores that the plant roots cannot reach, thus gaining access to essential nutrients that may be unavailable to the plant (Smith & Read, 2008). Mineral nutrients absorbed by mycorrhizal fungal hyphae are translocated to the plant root, where they are released to the host cell across specialized interfaces (Balestrini & Bonfante, 2005, 2014) and normally exchanged with photosynthesis-derived carbon. The uptake of phosphorus and nitrogen and their transfer to the mycorrhizal host plant have been extensively investigated (Bucher et al., 2014; Casieri et al., 2013), whereas much less is known about S uptake by mycorrhizal fungi and transfer to the host plant (Giovannetti et al., 2014).

Fungi can absorb inorganic S as sulfate through sulfate permeases belonging to the SulP family, although alternative S sources can be also exploited (Linder, 2018; Traynor et al., 2019). Mansouri-Bauly et al. (2006) identified two sulfate transporters in the ectomycorrhizal fungus *Laccaria bicolor*, but data on other mycorrhizal fungi are scanty and S metabolism in fungi in general has been investigated in a limited number of species (Piłsyk & Paszewski, 2009). Fungi can assimilate S through a reductive sulfate assimilation pathway slightly different from the one described in plants. After transport into the cell, sulfate is reduced to APS, which is then phosphorylated by an APS kinase to form PAPS. A PAPS reductase then releases sulfite from PAPS, which is reduced to sulfide by a sulfite reductase (Traynor et al., 2019). In fungi, the reductive sulfate assimilation pathway is therefore linear and includes PAPS as an intermediate.

Sulfur transfer to the host plant by mycorrhizal fungi has been investigated in arbuscular mycorrhiza, by far the most common and best studied mycorrhizal symbiosis. Arbuscular mycorrhizal colonization substantially improved the S status of the host in many plant species, especially under low-sulfate conditions (Allen & Shachar-Hill, 2009; Casieri et al., 2012; Sieh et al., 2013; Wu et al., 2018). By using ^{35}S-labeled sulfate, Allen and Shachar-Hill (2009) demonstrated sulfate uptake by the fungus and transfer to the mycorrhizal roots. Following mycorrhizal colonization, the SULTR1;1 and SULTR1;2 homologs from *Medicago truncatula* and *Lotus japonicus* were found to be expressed in cortical cells containing fungal arbuscules (Giovannetti et al., 2014), which are the site of nutrient exchange in arbuscular mycorrhiza. This finding suggests that, in arbuscular mycorrhiza, S is transferred to the plant cells mainly in the form of sulfate, although organic S forms may also be translocated (Allen & Shachar-Hill, 2009).

Information on S uptake and transfer to the host plant in other mycorrhizal types is very limited, and, to our knowledge, no previous studies have focused on S uptake and transfer in orchid mycorrhiza (OM). Plants in the Orchidaceae, one of the largest families of flowering plants, display minute seeds lacking storage reserves and an immature embryo, which need carbon and other nutrients for germination and development of a unique postembryonic structure called protocorm (Smith & Read, 2008). Orchid mycorrhiza represents therefore an unusual symbiosis because, at least in the early plant developmental stages, the mycorrhizal fungus transfers organic carbon to

the host plant in addition to other nutrients (see in Cameron et al., 2006; Kuga et al., 2014; Smith & Read, 2008). Nutrient transfer in OM has been mainly studied in mycorrhizal protocorms, where plant cells colonized by intracellular fungal coils, or pelotons, are considered the site of nutrients transfer. Kuga et al. (2014) demonstrated ^{13}C and ^{15}N transfer to *Spiranthes sinensis* protocorms colonized by the OM fungus *Ceratobasidium* sp. using secondary ion mass spectrometry (SIMS). Here, we used SIMS to investigate ^{34}S transfer from an isolate of the OM fungus *Tulasnella calospora* to mycorrhizal protocorms of its host plant *Serapias vomeracea*. ^{13}C and ^{15}N transfer were also measured for comparison. To elucidate the molecular bases of S uptake and transfer in OM, the expression profile of plant and fungal genes potentially involved in S metabolism was investigated in asymbiotic and symbiotic conditions.

RESULTS

Uptake of sulfate and other elements by *Tulasnella calospora* and transfer to mycorrhizal protocorms of the orchid host *Serapias vomeracea*

Stable isotope tracers above natural abundances were detected in the intracellular hyphae colonizing mycorrhizal protocorm cells, as shown in the ratio images of the tracers r13C, rC15N, and r34S (Figure 1). In particular, the ratio images showed that the three stable isotopes highly labeled the peloton hyphae in the colonized protocorm cells, but not the fungal dead masses (Figure 1f–h). The average values of ^{13}C, ^{15}N, and ^{34}S tracer in the fungal hyphae are reported in Table 1. Because the natural abundance is about 1% for ^{13}C, 0.36% for ^{15}N, and 0.4% for ^{34}S, the expected values of $r^{13}C \times 100$, $rC^{15}N \times 1000$, and $r^{34}S \times 100$ are about 1, 4, and 4, respectively. The significantly higher average values in the fungal pelotons for all isotopes (Table 1) indicate that the fungal hyphae absorbed the labeled tracers (as ^{34}S-labeled sulfate, ^{13}C-labeled glucose, and ^{15}N-labeled ammonium nitrate) from the agar medium and translocated them to the orchid protocorm.

In colonized protocorm cells, the plant nuclei showed contents above natural abundance for all isotopes, with ratio values that were significantly correlated with the ratio values of $rC^{15}N$ and $r^{34}S$ measured, within the same cells, in the fungal hyphae (Figure 2). These results on the host nuclei indicate that tracers translocated by the fungal hyphae in the mycorrhizal protocorms were transferred to the host cell. The stable isotope imaging showed that $r^{34}S$, $r^{13}C$, and $rC^{15}N$ measured in the plant nuclei were higher than the values of natural abundances not only in the colonized cells but also in uncolonized protocorm cells close to mycorrhizal cells or in the cortical and meristematic region (Table 1). In particular, the highest isotopes ratios were measured in the plant nuclei in the uncolonized cells next to the colonized cells (Figure 1b–d), with values significantly higher when compared to those of the other cells, both uncolonized and colonized (Figure 3). Altogether, these results indicate that stable isotope-labeled compounds, once transferred from the fungal hypha to the host cell, were translocated in other protocorm regions.

A significant linear correlation was observed between different isotope tracers in both the intracellular fungal hyphae and the plant nuclei of colonized and uncolonized cells. The strongest correlation, both in the fungal and plant structures, was between $rC^{15}N$ and $r^{34}S$ (Figure 4). These results would indicate that compounds containing N and S were translocated at the same rate, or that N and S were both present in the same translocated molecule.

Identification and expression of fungal genes involved in S uptake and assimilation

The complete genome sequence of *T. calospora* (Kohler et al., 2015), available on the MycoCosm portal (http://genome.jgi.doe.gov/Tulca1/Tulca1.home.html), was searched for fungal genes potentially involved in S uptake and metabolism. Specifically, a search using the keyword "sulfate" led to the identification of protein-coding genes potentially involved in the transport, transformation, or usage of this element (Table 2). Three genes coding for putative sulfate transporters of the SulP family (*TcSULP1*, *TcSULP2*, *TcSULP3*) were identified, showing homology with sequences of putative transporters and permeases of other basidiomycetes. The best BLASTX hits for all three genes were putative sulfate anion transporters (Table 2).

These *T. calospora* genes were found to be differentially expressed in the mycorrhizal symbiosis in a previous RNAseq experiment (Fochi, Chitarra, et al., 2017). Here, RT-qPCR were here used to investigate their expression in the free-living mycelium (FLM), in the fungal mycelium grown on the substrate next to mycorrhizal protocorms (MYC), and in the mycelium inside mycorrhizal protocorms (SYMB). Expression measured by RT-qPCR, with respect to expression in FLM, is reported in Table S4, and a graphical representation is provided in the heatmap in Figure 5. An opposite expression pattern was revealed for *TcSULP2*, whose expression was strongly down-regulated in MYC samples and up-regulated in SYMB samples, and the other two *TcSULP* genes, both up-regulated in MYC samples and down-regulated in SYMB samples (Figure 5). Five additional fungal genes known to be involved in the different steps of the S reductive pathway were selected in the genome of *T. calospora*, namely a gene coding for a putative ATP sulfurylase (*TcATPSul*) involved in the production of adenosine 5′-phosphosulfate (APS), two genes coding for putative APS kinases (*TcAphk 1* and *TcAphk2*), that phosphorylate APS in 3′-phosphoadenosine 5′-phosphosulfate (PAPS), a putative PAPS reductase (*TcPSRed*), that catalyzes the formation of sulfite ions, and a gene coding for a putative sulfite reductase involved in the last step of reduction in sulfite to sulfide

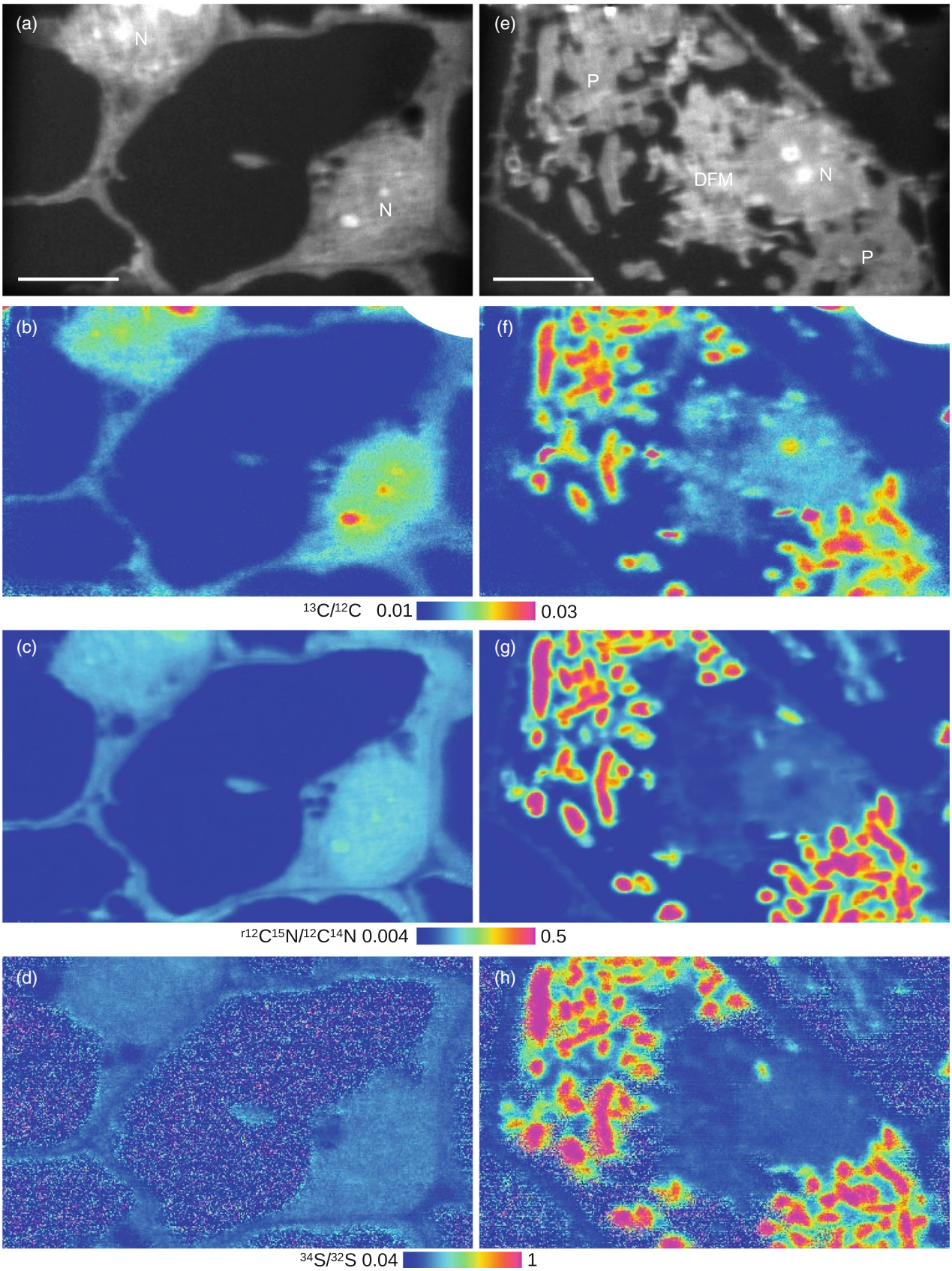

Figure 1. Secondary ion mass spectrometry imaging of a symbiotic protocorm of *Serapias vomeracea* associated with *Tulasnella calospora*. ^{13}C-glucose, $^{15}NH_4{}^{15}NO_3$, and $Mg^{34}SO_4$ were added only to extraradical hyphae and incubated for 6 days. Isotopograph of $^{12}C^{14}N$ (a,e), $^{13}C/^{12}C$ (b,f), $^{12}C^{15}N/^{12}C^{14}N$ (c,g), and $^{34}S/^{32}S$ (d,h).
(a-d) Uncolonized cortical cells next to colonized region.
(e-h), Colonized cell with a fungal peloton and a dead fungal mass from previous colonization. DFM, dead fungal mass; N, plant nucleus; P, peloton. The lowest color indexes are the value of the natural abundance of each isotope. Bars, 20 μm.

Table 1 ^{13}C, ^{15}N, and ^{34}S tracer values of *Serapias vomeracea* protocorm symbiotically germinated with *Tulasnella calospora* (6 days labeling)

		Plant nuclei			
			Uncolonized cells		
	Fungal pelotons	Colonized cells	Cortical next to the colonized region	Cortical and meristem	All
Number of images	30	18	4	4	26
$^{13}C/^{12}C \times 100$	2.26 ± 0.50	1.48 ± 0.10	1.76 ± 0.12	1.48 ± 0.08	1.52 ± 0.14
$^{12}C^{15}N/^{12}C^{14}N \times 1000$	322.35 ± 97.80	78.31 ± 12.03	148.63 ± 13.54	77.88 ± 10.25	89.06 ± 28.10
$^{34}S/^{32}S \times 100$	68.39 ± 16.18	18.33 ± 1.47	23.66 ± 1.54	16.40 ± 1.10	18.56 ± 2.59

An aqueous mixture of tracers (1% ^{13}C-glucose, 0.2% $^{15}NH4^{15}NO3$, 0.1% $Mg^{34}SO4$) was added to the external hyphae and incubated for 6 days.
r13C, $^{13}C/^{12}C$; rC15N, $^{12}C^{15}N/^{12}C^{15}N$; r34S, $^{34}S/^{32}S$. The expected values used in this study for the natural abundance of the isotopes (^{13}C, 1%; ^{15}N, 0.36%; ^{34}S, 4%): r13C × 100 = *c.* 1; rC15N × 1000 = *c.* 4; r34S × 100 = *c.* 4.
Average ± SD.

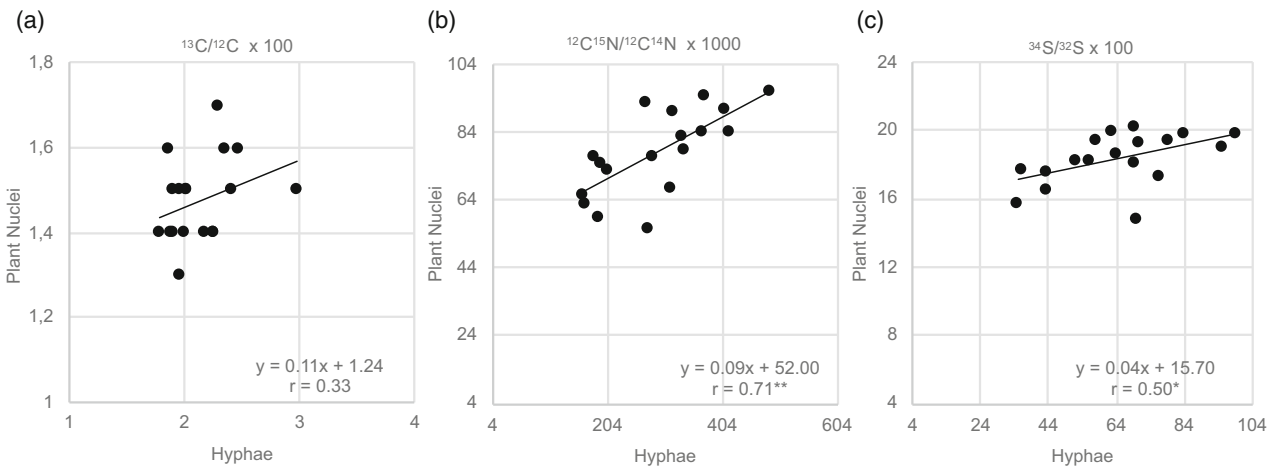

Figure 2. Scatter plots and Pearson's correlation coefficient showing the relationship between the isotope ratios measured in the fungal peloton hyphae and in the plant nucleus of the same colonized protocorm cell of *Serapias vomeracea*.
(a) $^{13}C/^{12}C \times 100$.
(b) $^{12}C^{15}N/^{12}C^{14}N \times 1000$.
(c) $^{34}S/^{32}S \times 100$. $n = 18$. Pearson's coefficient correlation, both side: *, $P < 0.05$; **, $P < 0.01$.

ions. The transcripts of these genes all showed a similar expression pattern in the fungal mycelium, with a significant down-regulation in MYC samples, with respect to FLM, and a strong up-regulation in SYMB samples (Table S4 and Figure 5).

A gene encoding a putative sulfite efflux pump (*TcSul*), required for the secretion of sulfite as a reducing agent, was also selected in the genome of *T. calospora* as a gene putatively involved in S transport between partners. This gene was significantly up-regulated in both the MYC and SYMB samples, as compared to FLM (Figure 5).

Selection and gene expression analysis of plant transcripts putatively involved in S uptake and assimilation

RT-qPCR was also performed on plant genes involved in S uptake, transport, and assimilation. The genome sequence of *S. vomeracea* is currently unavailable, and genes of interest were therefore selected from the RNA-Seq data

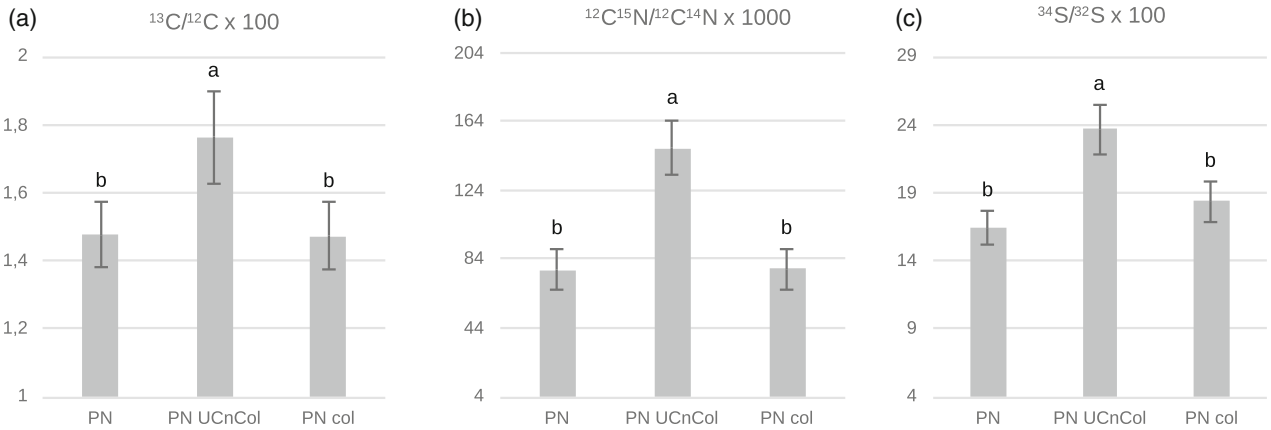

Figure 3. SIMS ROI analysis plant nuclei in a symbiotic protocorm of *Serapias vomeracea* associated with *Tulasnella calospora*. All isotope ratios of plant nuclei in meristematic cells (PN), colonized cells (PN col), and uncolonized cells next to colonized region (PN UCnCol) were higher than the natural abundances and reveal accumulation of elements of fungal origin. Among them, PN UCnCol shows highest elevations of all tracers. Tukey–Kramer multiple comparison, the different letters indicate statistical difference between the samples. (a) $^{13}C/^{12}C \times 100$. (b) $^{12}C^{15}N/^{12}C^{14}N \times 1000$. (c) $^{34}S/^{32}S \times 100$.

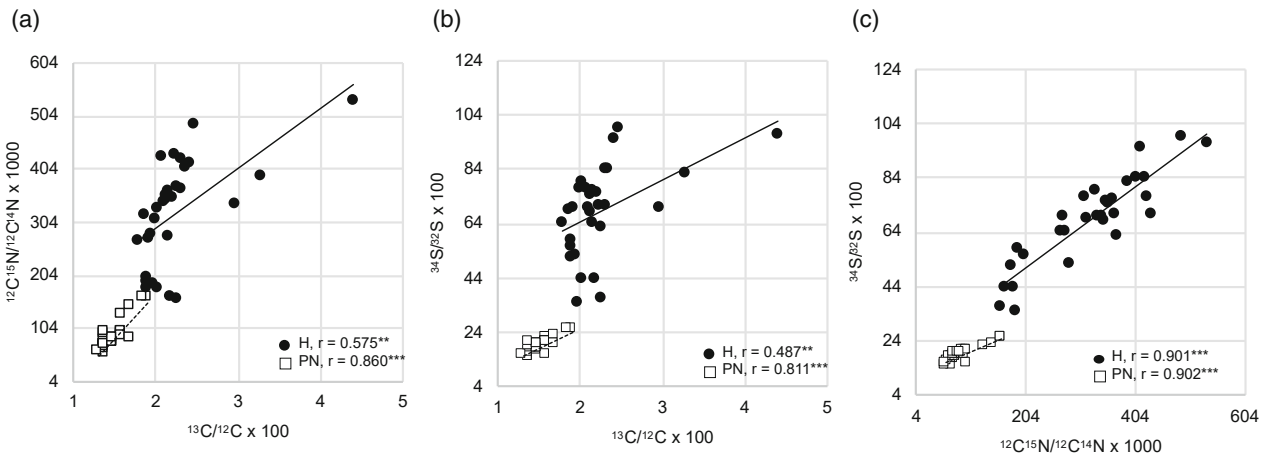

Figure 4. Scatter plots and Pearson's correlation coefficient showing the relationship between different isotope ratios measured in the same structure, either fungal peloton hyphae or plant nuclei, in *Serapias vomeracea* protocorm cells colonized by *Tulasnella calospora*.
(a) $^{13}C/^{12}C \times 100$ and $^{12}C^{15}N/^{12}C^{14}N \times 1000$.
(b) $^{13}C/^{12}C \times 100$ and $^{34}S/^{32}S \times 100$.
(c) $^{12}C^{15}N/^{12}C^{14}N$ and $^{34}S/^{32}S \times 1000$. ●, pelotons; □, plant nuclei. *, $P < 0.05$; **, $P < 0.01$; ***, $P < 0.001$.

obtained by Fochi, Chitarra, et al. (2017) for this species and from a cDNA library obtained by 454 GS-FLX Titanium pyrosequencing (Perotto et al., 2014). Nine *S. vomeracea* sequences annotated as sulfate transporters (Table 3) were compared with sulfate transporters already described in the literature. Phylogenetic analysis (Figure 6) showed that six *S. vomeracea* sequences (*SvST2, SvST4, SvST5, SvST6, SvST7*, and *SvST8*) clustered with Group 3 plant sulfate transporters (SULTR 3) together with several sequences from other orchids, one sequence (*SvST3*) with Group 1 SULTRs and two sequences (*SvST1, SvST9*) with Group 4 SULTRs.

As compared to asymbiotic protocorms, analysis of the transcript expression profiles in the mycorrhizal protocorms (Table S5 and Figure 6) showed strong up-regulation of the *S. vomeracea* sulfate transporters identified as Group 3 SULTRs by phylogenetic analysis (Figure 6a), except for *SvST4* that was not significantly regulated. SvST3, a sulfate transporter clustering with Group 1 SULTRs, reported to be localized on the plasma membrane (Kopriva et al., 2016, 2019), showed no significant differences in gene expression between symbiotic and asymbiotic protocorms (Table S5 and Figure 6b). SvST9, one of the two sulfate transporters clustering in Group 4 SULTRs, reported to be efflux transporters on the tonoplast (Takahashi, 2019), was strongly up-regulated in symbiotic conditions, the other one (*SvST1*) being not differentially regulated (Table S5 and Figure 6b).

Table 2 List of the *T. calospora* sequences analyzed in this work

ID Sequence[a]	Sequence name	Best Blastx hit	Accession	% similarity	E-value
20 907	*TcSULP1*	Sulfate anion transporter [*Dichomitus squalens*]	XP_007370085.1	60.19%	0.0
20 008	*TcSULP2*	Sulfate anion transporter [*Rhizoctonia solani*]	XP_043176186.1	63.24%	0.0
215 409	*TcSULP3*	Sulfate anion transporter [*Rhizoctonia solani*]	XP_043183174.1	58.79%	0.0
14 111	*TcATPSUL*	ATP sulfurylase [*Fomitiporia mediterranea*]	XP_007266540.1	80.00%	0.0
75 899	*TcAphK1*	Adenylylsulfate kinase [*Dichomitus squalens*]	XP_007361681.1	78.89%	$2e^{-113}$
33 232	*TcAphK2*	Adenylylsulfate kinase [*Dichomitus squalens*]	XP_007361681.1	87.84%	$1e^{-40}$
241 285	*TcPsRed*	Phosphoadenylyl-sulfate reductase [*Trametes versicolor*]	XP_008035525.1	64.88%	$3e^{-108}$
65 027	*TcSR*	Assimilatory sulfite reductase [*Fomitiporia mediterranea*]	XP_007268242.1	52.88%	0.0
20 203	*TcSul*	Plasma membrane sulfite pump involved in sulfite metabolism [*Pleurotus ostreatus*]	XP_036630505.1	37.06%	$4e^{-90}$

[a]Protein ID from https://mycocosm.jgi.doe.gov.

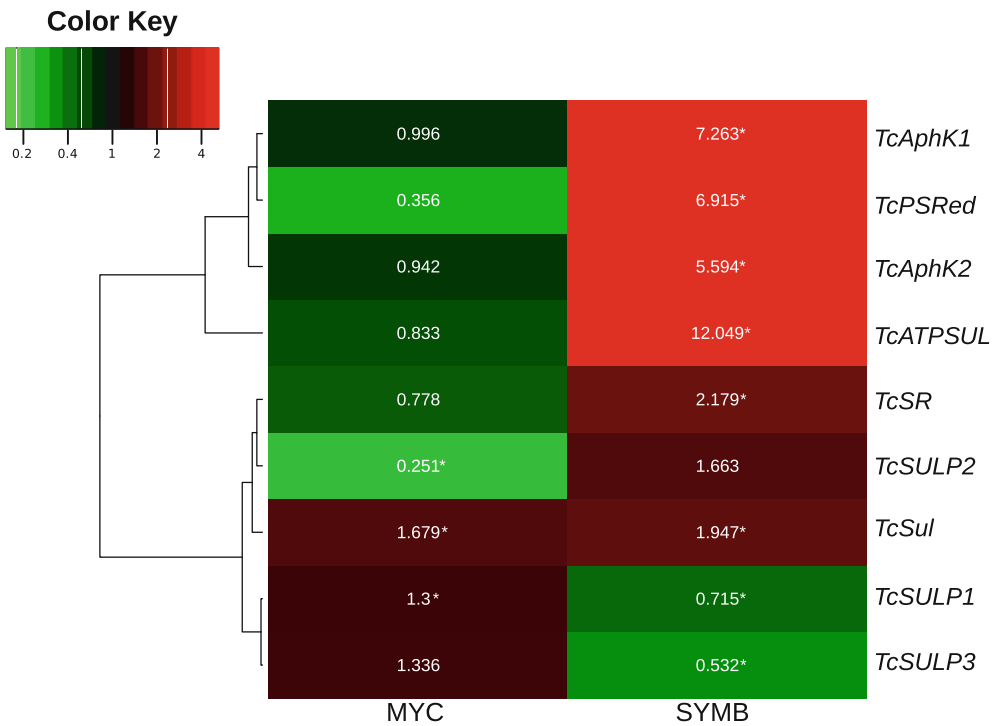

Figure 5. Heat map representation of the fungal transcript levels with a hierarchical clustering in MYC and SYMB samples. Expression levels are reported as fold change (FLM used as reference) and are colored green for low intensities (down-regulation) and red for high intensities (up-regulation). In order: adenylyl-sulfate kinase (*TcAphK1*), phosphoadenylyl-sulfate reductase (*TcPsRed*), adenylylsulfate kinase (*TcAphK2*), ATP sulfurylase (*TcATPSUL*), sulfite reductase (*TcSR*), sulfate transporter (*TcSULP2*), sulfite efflux pump (*TcSul*), and sulfate transporters (*TcSULP1* and *TcSULP3*). Asterisks indicate significant differences ($P < 0.05$) compared with the control (FLM) as inferred by the Pairwise Fixed Reallocation Randomization Test© performed by using REST©.

Seven plant genes showing homology with enzymes involved in the reductive sulfate assimilation pathway or in the sulfation of secondary metabolites (Table 3) were further identified in the available *S. vomeracea* transcriptomes (Fochi, Chitarra, et al., 2017; Perotto et al., 2014). Gene expression analysis (Table S5 and Figure 6b) revealed that none of the plant genes involved in the sulfate reductive assimilation pathway was significantly regulated in symbiosis, whereas the sulfotrasferase gene *SvSTRF*, putatively involved in the sulfation of secondary metabolites, was strongly up-regulated in mycorrhizal protocorms (Table S5 and Figure 6b).

Laser microdissection (LMD) and gene expression in mycorrhizal protocorms

To investigate cell-type specific expression of plant and fungal genes potentially involved in sulfate uptake, transport, and assimilation, about 1300 protocorm cells either

Table 3 List of the *S. vomeracea* sequences analyzed in the current work

ID Sequence	Sequence name	Best Blastx hit	Accession	% similarity	E-Value
R2_C16339[b]	*SvST1*	Probable sulfate transporter 4.2 [*Phalaenopsis equestris*]	XP_020585462.1	87.76%	$4e^{-50}$
R2_Rep_C202[b]	*SvST2*	Probable sulfate transporter 3.4 [*Dendrobium catenatum*]	XP_020699429.1	75.86%	$4e^{-36}$
R2_Rep_C5242[b]	*SvST3*	Sulfate transporter 1.3-like [*Phoenix dactylifera*]	XP_008780888.2	79.67%	$2e^{-97}$
R2_C13484[b]	*SvST4*	Sulfate transporter 3.1 [*Dendrobium catenatum*]	XP_020699282.1	69.47%	$3e^{-37}$
TRINITY_DN68835_c1_g2_i1[a]	*SvST5*	Probable sulfate transporter 3.4[*Dendrobium catenatum*]	XP_020699429.1	82.89%	$2e^{-80}$
TRINITY_DN63650_c0_g1_i1[a]	*SvST6*	Probable sulfate transporter 3.4 [*Phoenix dactylifera*]	XP_008793448.1	71.23%	$7e^{-164}$
TRINITY_DN63650_c0_g2_i1[a]	*SvST7*	Probable sulfate transporter 3.4 [*Dendrobium catenatum*]	XP_020690822.1	77.39%	$2e^{-53}$
TRINITY_DN76349_c3_g11_i1[a]	*SvST8*	Probable sulfate transporter 3.4 [*Dendrobium catenatum*]	XP_020699429.1	72.22%	$2e^{-52}$
TRINITY_DN63650_c0_g4_i1[a]	*SvST9*	Probable sulfate transporter 3.3 *[Phalaenopsis equestris*]	XP_020585326.1	46.55%	$1e^{-28}$
TRINITY_DN69207_c1_g1_i1[a]	*SvATPSul*	ATP sulfurylase 1, chloroplastic [*Phalaenopsis equestris*]	XP_020586112.1	87.04%	0.0
TRINITY_DN70992_c0_g1_i2	*SvAPSKin2*	Adenylyl-sulfate kinase 3 [*Dendrobium catenatum*]	XP_020689777.1	73.61%	$2e^{-142}$
TRINITY_DN58139_c0_g1_i1	*SvAPSRed1*	5′-adenylylsulfate reductase 3, chloroplastic [*Dendrobium catenatum*]	XP_020699460.1	77.51%	0.0
TRINITY_DN76001_c0_g1_i1	*SvSR2*	Sulfite reductase [ferredoxin], chloroplastic [*Dendrobium catenatum*]	XP_020698352.1	88.21%	0.0
TRINITY_DN74740_c3_g1_i1	*SvSTRF*	Flavonol 3-sulfotransferase-like [*Phalaenopsis equestris*]	XP_020575587.1	62.12%	$1e^{-110}$
R2_C9449[b]	*SvAPSRed2*	5′-adenylylsulfate reductase-like 3 [*Phalaenopsis equestris*]	XP_020581002.1	61.62%	$1e^{-77}$
R2_C11840[b]	*SvAPSRed3*	5′-adenylylsulfate reductase-like 5 [*Phalaenopsis equestris*]	XP_020574787.1	63.33%	$8e^{-60}$
R2_Rep_C7777[b]	*SvSR1*	Sulfite reductase 1 [ferredoxin], chloroplastic [*Dendrobium catenatum*]	XP_028554576.1	80.26%	$1e^{-34}$

[a]From RNA-seq by Illumina HiSeq2000 (Fochi, Chitarra, et al., 2017).
[b]From cDNA library by 454 GS-FLX Titanium pyrosequencing (Perotto et al., 2014).

with or without visible fungal pelotons were collected by LMD for each of the three biological replicates and used for RNA extraction and One-Step RT-PCR. RNA samples were amplified by RT-PCR using primers specific for the *T. calospora* elongation factor *TcEF-1α*, to detect the presence of the fungus in the LMD collected cells (Figure 7). Absence of an amplified product in the RT minus reactions excluded genomic DNA contamination (not shown). No differences in plant gene expression were observed between the two microdissected cell-type populations but, unfortunately, transcripts corresponding to the fungal housekeeping gene *TcEF-1α* could be amplified in samples of LMD plant cells that did not contain visible fungal coils. The amplification of fungal transcripts in apparently uncolonized cells may be due to the fact that small pelotons, either very young or already collapsed, may go undetected in some cortical cells during microdissection. This difficulty in the collection of specific cell types was already reported for orchid mycorrhizal roots by Fochi, Falla, et al. (2017). To avoid presenting a biased data, only results from colonized cells have been presented here. The successful amplification of *TcSULP2*, *TcATPSul*, *TcAphK1*, *TcAphK2*, *TcSR*, and *TcSul* transcripts in at least two replicates of the colonized protocorm cells agreed with the expression in symbiosis revealed by the RT-qPCR analysis. The two sulfate permeases *TcSULP1* and *TcSULP3*, which appeared to be down-regulated in the whole protocorms by RT-qPCR, could not be amplified in any of the RNA samples from colonized LMD cells, thus suggesting a low level of transcripts in the symbiotic stage. The only discrepancy with the quantitative data on the protocorms (Figure 5 and Table S4) was for *TcPsRed*. This result could be mainly due to differences in the RNA extraction protocols and amplification method (One-Step RT-PCR *vs* RT-qPCR). Additionally, since RT-PCR has been performed on RNA extracted from subpopulations of intracellular fungal coils, we cannot exclude that *TcPsRed* might be exclusively expressed in intercellular hyphae inside the protocorms, or in a specific step of fungal coil development. The latter hypothesis would explain the absence of transcripts in some of the colonized cell

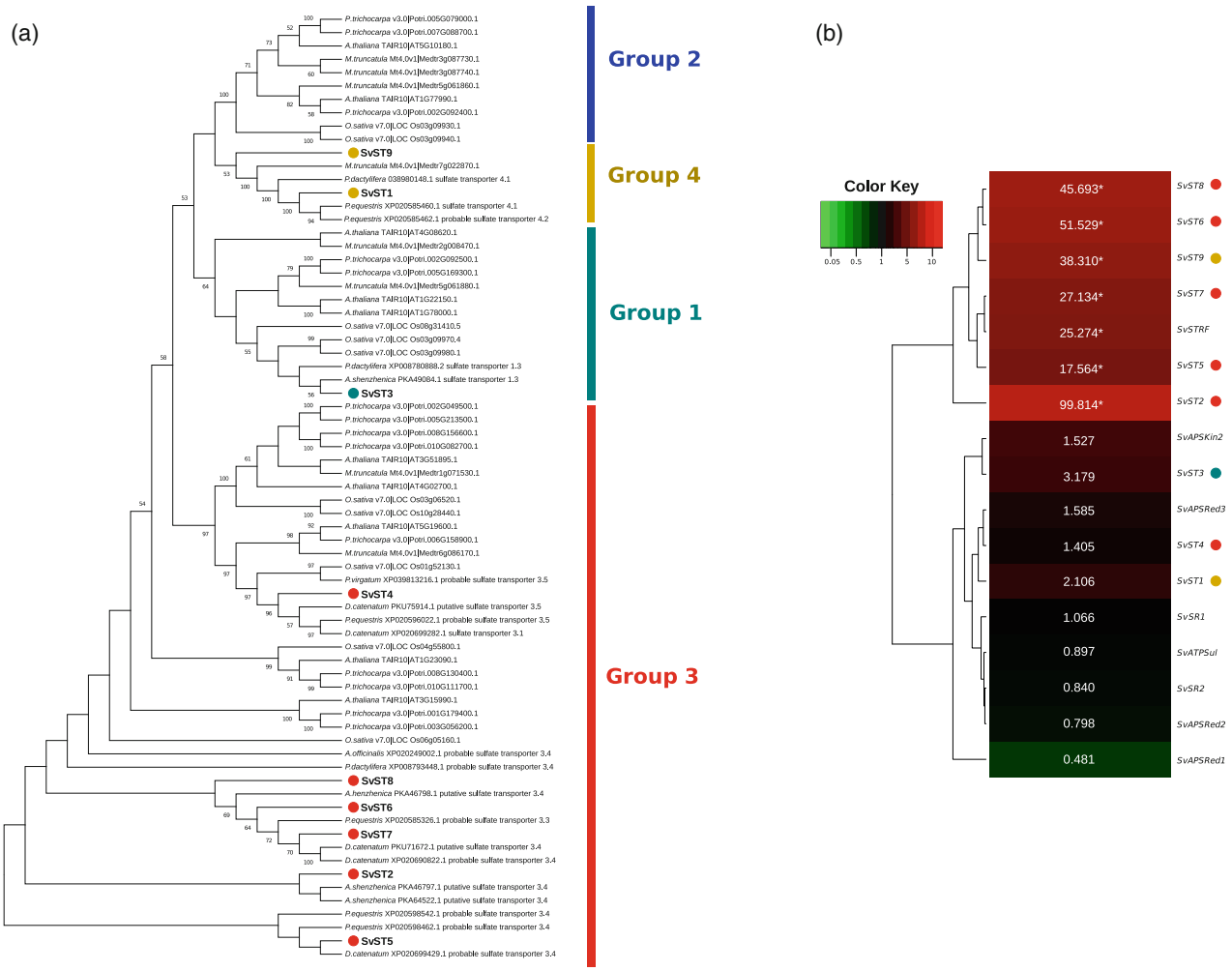

Figure 6. Phylogenetic analyses of plant sulfate transporters and gene expression on plant sulfur metabolism genes.
(a) Phylogenetic analysis of sequences putatively coding for *S. vomeracea* sulfate transporters (*SvST1*, *SvST2*, *SvST3*, *SvST4*, *SvST5*, *SvST6*, *SvST7*, *SvST8*, and *SvST9*) as a bootstrap consensus tree. Only bootstrap values >50% are showed.
(b) Heat map representation of the plant transcript levels with a hierarchical clustering in symbiotic protocorms. Expression levels are reported as Fold Change (asymbiotic protocorms used as reference) and are colored green for low intensities (down-regulation) and red for high intensities (up-regulation). *SvST8*, *SvST6*, *SvST9*, and *SvST7* (sulfate transporters), *SvSTRF* (sulfotrasferase), *SvST5* and *SvST2* (sulfate transporters), *SvAPSKin2* (adenylylsulfate kinase), *SvST3* (sulfate transporter), *SvAPSRed3* (5′-adenylylsulfate reductase), *SvST4* and *SvST1* (sulfate transporters), *SvSR1* (sulfite reductase), *SvATPSul* (ATP sulfurylase), *SvSR2* (sulfite reductase), *SvAPSRed2* and *SvAPSRed1* (5′-adenylylsulfate reductases). Asterisks indicate significant differences ($P < 0.05$) compared with the control (ASYMB) as inferred by the Pairwise Fixed Reallocation Randomization Test© performed by using by REST©.

replicates also observed for other fungal transcripts. By using primer sets designed for plant transcripts, RT-PCR with specific primers for the *S. vomeracea* housekeeping gene (the elongation factor *SvEF-1α*) yielded an amplified fragment of the expected size in all RNA samples (Figure 7). Sulfate transporters *SvST2, SvST3, SvST5, SvST6, SvST7*, and *SvST9* showed amplification in at least two of the three biological replicates (Figure 7), while *SvST1* did not show amplification in any of the samples (not shown). Most transcripts corresponding to plant genes involved in S assimilation (*SvSR1*, *SvSR2*, *SvATPSul*, *SvAPSKin2*, *SvAPSRed1*, *SvSTRF*) appeared not significantly up-regulated in RT-qPCR (Figure 6b and Table S5), but they could be detected in colonized cells.

DISCUSSION

Mycorrhizal fungi can assist plants in the uptake of macronutrients essential for their metabolism and growth, and a role in S uptake, especially under low-sulfate conditions, has been demonstrate in the ubiquitous arbuscular mycorrhizal fungi (Allen & Shachar-Hill, 2009; Giovannetti et al., 2014; Ma et al., 2022; Sieh et al., 2013; Wu et al. 2018). The role of ectomycorrhizal fungi in S nutrition has not been extensively investigated, but they are

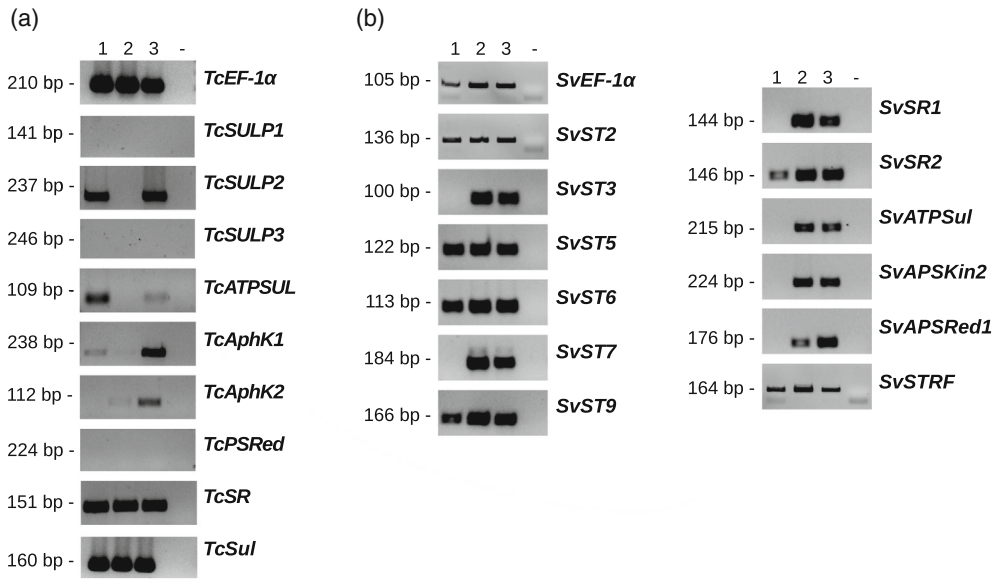

Figure 7. One-Step RT-PCR of laser microdissected mycorrhizal cells from *S. vomeracea* protocorms using fungal (a) and plant (b) primers. Numbers (1), (2), and (3) correspond to the three biological replicates, while (−) correspond to the negative control. In (a), tested genes: *TcEF-1α* (elongation factor), *TcSULP2* (sulfate transporter), *TcATPSUL* (ATP sulfurylase), *TcAphK1* and *TcAphK2* (adenylylsulfate kinases), *TcSR* (sulfite reductase), and *TcSul* (sulfite efflux pump). In (b), tested genes: *SvEF-1α* (elongation factor), sulfate transporters (*SvST2, SvST3, SvST5, SvST6, SvST7* and *SvST9*), *SvSR1* and *SvSR2* (sulfite reductase), *SvATPSul* (ATP sulfurylase), *SvAPSKin2* (adenylylsulfate kinase), *SvAPSRed1* (5′-adenylylsulfate reductase), and *SvSTRF* (sulfotrasferase).

suggested to contribute to the regulation of sulfate uptake by the host (Mansouri-Bauly et al., 2006).

Here, we showed that an orchid mycorrhizal fungus in the genus *Tulasnella* can assist protocorms of the host plant *Serapias vomeracea* not only in C and N nutrition, as already demonstrated in other orchid species (see in Kuga et al., 2014; Smith & Read, 2008), but also in S nutrition. Compounds labeled with stable isotopes (^{34}S-sulfate, ^{13}C-glucose and ^{15}N- ammonium nitrate) were taken up by the external mycelium of *T. calospora* and translocated to the mycorrhizal protocorms *via* the fungal hyphae. Intracellular fungal hyphae accumulated high amounts of stable isotopes, whereas collapsed fungal masses were not labeled in our study. This is likely because they were already non-functional in nutrient transport when labeling was applied to the external medium, as fungal pelotons in mycorrhizal protocorm cells undergo a rapid turnover culminating in hyphal degeneration and collapse (Uetake et al., 1992). Labeling of plant nuclei indicate that, inside the mycorrhizal protocorms, labelled compounds were transferred from the intracellular hyphae to the host cells and further allocated to the uncolonized cells and the meristem. Interestingly, plant nuclei in uncolonized cells next to the colonized region accumulated more stable isotopes than nuclei in peloton harboring cells, suggesting a higher cellular activity than the colonization events, such as reported in pathogenic infections and arbuscular mycorrhizal colonization (Balestrini et al., 1992; Deslandes & Rivas, 2011). In which chemical form these stable isotopes reach the neighboring cells once they are transferred from the fungal pelotons to the colonized cells, and by which route (symplastic or apoplastic), remains to be elucidated.

The *T. calospora* sulfate permease TcSULP1 may be involved in the uptake of sulfate from the substrate, as it was significantly up-regulated in the fungal mycelium outside the mycorrhizal protocorms and down-regulated inside the orchid protocorms. A similar trend was also found for TcSULP3, although gene regulation was significant only inside the protocorm. In addition to mycorrhizal fungi, some fungal endophytes can improve the host plant nutritional status (Baron & Rigobelo, 2022). The genus *Serendipita* (Serendipitaceae, Basidiomycetes) is intriguing because it harbors well-established fungal endophytes but also species forming orchid mycorrhiza (Oktalira et al., 2021). *Serendipita indica* is a well-characterized endophyte that displays nutrient transportation abilities (Card et al., 2016). This fungal endophyte enhances S uptake in maize plants thanks to the activity of a high-affinity sulfate transporter SiSulT (Narayan et al., 2021). Knockdown strains lacking SiSulT failed to support plant growth under low-sulfate conditions, demonstrating the importance of this fungal transporter (Narayan et al., 2021). The importance of the two *T. calospora* sulfate transporters TcSULP1 and TcSULP3 in assisting the orchid host in S uptake remains to be established.

Plant roots acquire S directly from soil in the form of sulfate, thanks to sulfate transporters belonging to Group 1, represented in *Arabidopsis* by SULTR1;1 and SULTR 1;2

(Takahashi et al., 2000). In symbiotic plant–fungus interactions, nutrients taken up from the substrate by the external fungal hyphae are translocated to the host, where they are released across specialized plant–fungus interfaces (Ivanov et al., 2019). In arbuscular mycorrhizal *Lotus japonicus*, the LjSULTR1;2 promoter was activated in cortical root cells containing arbuscules, the highly branched intracellular fungal structures typical of this symbiosis, suggesting that S is transferred as sulfate from the fungus to the host plant across the plant-derived periarbuscular membrane (Giovannetti et al., 2014). Translocation of S to the respective host plants in the form of sulfate has been also suggested for the ectomycorrhizal fungus *Laccaria laccata* (Mansouri-Bauly et al., 2006) and the fungal endophyte *S. indica* (Narayan et al., 2021).

The form of S translocated to the plant in orchid mycorrhiza is currently unknown, but results of transcriptomic experiments in this study suggest that S is at least in part translocated as an organosulfur compound. In particular, the strong activation of the sulfate reductive assimilation pathway in the fungus *T. calospora* when inside the mycorrhizal protocorm, together with the lack of a significant induction of the reductive assimilation pathway in the orchid host when in symbiosis, suggest that at least part of S is taken up as sulfate from the substrate and reduced by the fungus before S translocation to the plant.

The genome sequence of *S. vomeracea* is not currently available and the set of plant genes tested in this study as being involved in sulfate uptake and metabolism likely provides an incomplete picture of S metabolism in this orchid species. However, transcripts were selected from transcriptomic experiments on mycorrhizal protocorms, ensuring that genes expressed in symbiosis should be represented in the tested gene set. This was confirmed by LMD experiments, where most of the plant genes analyzed could be revealed in at least two of the three biological replicates. It was therefore intriguing and consistent with the hypothesis of organosulfur compounds being transferred to the plant, that the only Group 1 sulfate transporter identified (*SvST3*) was slightly but not significantly induced in mycorrhizal protocorms, as tested by RT-qPCR.

Interestingly, SIMS data indicate a very strong linear correlation between ^{15}N and ^{34}S labeling in both the intracellular fungal hyphae and the plant nuclei. The most likely explanation of these results is that organic compound(s) containing both N and S, like the S-amino acids cysteine and methionine, are translocated from the fungus to the plant, although we cannot exclude the possibility that separate compounds containing either N or S are translocated to the host at the same rate and/or that separately transferred N and S are used inside the same molecule formed in the host cell. Although sulfate seems to be the main S compound translocated in arbuscular mycorrhiza, the S-amino acids cysteine and methionine were also suggested to be released from arbuscular mycorrhizal fungi to plant roots (Allen & Shachar-Hill, 2009).

Specific cysteine (or methionine) membrane transporters have been described in fungi, such as the high-affinity cysteine importer Yct1 in yeast (Kaur & Bachhawat, 2007), but it is unclear whether similar specific transporters exist in plants or whether a less specific transport of S-amino acids occurs through general amino acid permeases (Gigolashvili & Kopriva, 2014). Plants possess a high number of amino acid transporters, many of them potentially capable of transporting cysteine, at least *in vitro* (Lee et al., 2014).

Previous work on orchid mycorrhiza showed that plant amino acid transporters are strongly up-regulated in mycorrhizal orchid protocorms, as compared to asymbiotic conditions (Fochi, Chitarra, et al., 2017; Miura et al., 2018). These transporters have been suggested to be responsible for the uptake of nitrogen released by the fungus in the form of amino acids (Dearnaley & Cameron, 2017; Fochi, Chitarra, et al., 2017). Notably, transcripts coding for two general amino acids permease (AAPs) and a Lysine Histidine Transporter 1 (LHT1) accumulated specifically in *S. vomeracea* cells containing viable fungal coils of *T. calospora* (Fochi, Falla, et al., 2017). The AAPs transport a broad spectrum of amino acids (Yang et al., 2020), and it is therefore possible that they may facilitate S-amino acids uptake across the plant–fungus intracellular interface. On the other hand, S-amino acids may also be metabolized in the fungal cells to form tripeptides that can be then transported by plant oligopeptides transporters. Cysteine is involved in the formation of the tripeptide glutathione, and some members of the oligopeptide transporter (OPT) family indeed transport this compound (Cagnac et al., 2004; Zhang et al., 2016). Interestingly, many plant OPTs were found to be very strongly induced in mycorrhizal orchid protocorms (Fochi, Chitarra, et al., 2017; Miura et al., 2018), but their specificity and role remain to be established.

Most *S. vomeracea* Group 3 sulfate transporters were found to be strongly up-regulated in mycorrhizal protocorms, as compared to asymbiotic protocorms. In *Arabidopsis*, all five members of Group 3 sulfate transporters have been suggested to be redundantly involved in sulfate uptake across the envelope membrane of chloroplasts, the main site for sulfate reduction in plants (Takahashi et al., 2011), based on the SULTR3 localization on the chloroplast membrane (Chen et al., 2019) and decreased chloroplast sulfate uptake in single knockout mutants (Cao et al., 2013). If orchids receive S from the symbiotic fungal partner in an already reduced organic form, as suggested by the results of SIMS and transcriptomic experiments, reduction of sulfate in the plastids would be unnecessary, and plastid transporters would be expected to be down-regulated. However, other reports on Group 3 transporters suggest that members of this large group of sulfate transporters have variable subcellular localization and

functional roles (Takahashi, 2019). For example, SULTR3;5 is a plasma membrane protein expressed in the root vasculature of *Arabidopsis*, where is thought to aid SULTR2;1 in root-to-shoot sulfate translocation (Kataoka et al., 2004). Members of the SULTR3 family are also expressed in *Arabidopsis* seeds, where they are suggested to be involved in the distribution of sulfate and S metabolites during seed development (Zuber et al., 2010). Intriguingly, the *Arabidopsis* SULTR3;3 ortholog in *Oryza sativa* did not show transporting abilities *in vitro*, and mutation of the corresponding gene altered the accumulation of phosphate and sulfate in rice seedlings (Zhao et al., 2016), thus revealing unexpected interactions between P and S assimilation pathways in plants (Sacchi & Nocito, 2019). Thus, the roles of SULTR3 subfamily members are variable and may depend on localization, plant species, and/or development stage. Their strong up-regulation in orchid mycorrhizal protocorms requires therefore further investigations.

To summarize, we have demonstrated that mycorrhizal protocorms of the terrestrial orchid *S. vomeracea* are assisted in S nutrition by their symbiotic fungal partner *T. calospora*, as labeled ^{34}S could be translocated from the substrate to the protocorm cells *via* the fungal hyphae. As previously suggested for N (Fochi, Chitarra, et al., 2017), we suggest that S may be also transferred to the plant in a reduced organic form, such as an amino acid or a small peptide such as glutathione. Reduction of sulfate and nitrate is an energy demanding process that normally occurs in the chloroplasts of photosynthetic plants. In this respect, translocation of molecules containing already reduced N and S could be an advantage for achlorophyllous orchid protocorms, that rely completely on the fungal symbiont for their energy supply in the form of organic carbon, a strategy termed mycoheterotrophy (Hynson et al., 2013). It would be therefore interesting to investigate S metabolism in fully photosynthetic adult orchid stages, where the role of the mycorrhizal fungus in nutrient uptake is largely unknown. Recent studies suggest that many photosynthetic meadow orchid species, like *S. vomeracea*, acquire organic compounds from their associated fungi throughout their entire life cycle, though being simultaneously photosynthetic (Gebauer et al., 2016; Schiebold et al., 2017; Stöckel et al., 2014). This observation, together with the finding that most adult orchid species, including *S. vomeracea*, acquire N from their fungal partner (Liebel et al., 2010), suggests that organic N forms are also taken up by adult orchids. Up-regulation of some amino acid transporters in mycorrhizal roots of adult *Oeceoclades maculata* (Valadares et al., 2020) and *Limodorum abortivum* (Valadares et al., 2021) provides further support to the hypothesis of translocation of organic N forms in adult orchids. We have currently no information of S translocation in adult *S. vomeracea* plants because our work focused on the early stages of this orchid species. However, a situation in adult plants like the one suggested for N could be speculated also for S and deserves to be further investigated.

Research on S metabolism in plants has been mainly focused on S uptake and primary metabolism, whereas less attention has been paid to the PAPS branch of sulfate assimilation and the synthesis of sulfated compounds, despite their crucial roles in stress defense and signaling (Chan et al., 2019; Kopriva et al., 2012). Sulfotransferases (STRF) are involved in the transfer of the functional sulfo group to hydroxylated substrates using PAPS as the sulfate donor, and the *S. vomeracea* STRF significantly up-regulated in the mycorrhizal protocorms may be involved in the synthesis of S-containing secondary metabolites. We have currently no information on the nature and role of sulfated compounds in *S. vomeracea* and metabolomic investigations are ongoing, but it is worth noting that S compounds can play special roles in some orchid species. For example, the spider orchid *Caladenia crebra* produces sulfurous pheromone mimics to attract its male wasp pollinator (Bohman et al., 2017).

Our study provides a glimpse on S metabolism in mycorrhizal protocorms and poses intriguing questions on the strategies that orchids evolved to obtain reduced forms of essential nutrients from the fungus, at least during the achlorophyllous stages. Although the molecular mechanisms that regulate S sensing and homeostasis are far for being understood in plants (Li et al., 2020; Ristova & Kopriva, 2022), a further step in the understanding of the orchid- fungus interactions would be the identification of the mechanisms that regulate fungal S uptake and transfer to the plant in symbiosis.

MATERIALS AND METHODS

Gene expression analyses and laser microdissection

Growth of free-living mycelium

The fungal isolate used in this study was originally isolated from mycorrhizal roots of the terrestrial orchid *Serapias vomeracea* grown in meadows in Northern Italy (Girlanda et al., 2011) and deposited in the mycological collection of the University of Turin (MUT) with the accession number MUT 4178. To confirm the identity of this *Tulasnella sp.* isolate, genomic DNA was extracted for Internal transcribed spacer (ITS) sequencing. The mycelium was grown in 2% malt extract liquid medium at 25°C in the dark in 250 ml flasks under continuous stirring. Once the mycelium reached 2 cm in diameter, it was collected by using sterilized tweezers and stored at −20°C.

To obtain actively growing mycelium for symbiotic orchid seed germination, the fungal isolate was grown on 2% malt extract agar (MEA) at 25°C in the dark for 10 days.

For RNA extraction, a mycelial plug with a diameter of 6 mm was transferred onto a sterilized cellulose membrane placed in 9 cm Petri dishes on top of solid oat agar (OA) medium (0.3% oat flour, 1% agar), as described by Schumann et al. (2013). After 15 days of growth in the dark at 25°C, this free-living mycelium (FLM) was collected with a spatula, immediately frozen in liquid nitrogen, and stored at −80°C.

Tulasnella *genomic DNA extraction and ITS region sequencing*

Genomic DNA from fungal mycelium grown in liquid medium was extracted using DNeasy® Plant Mini Kit (Qiagen, Valencia, CA, USA) following the protocol with some modifications. Total genomic DNA was quantified using spectrophotometry (NanoDrop 1000; BioRad Laboratories, Hercules, CA, USA) and a PCR reaction with ITS1 and ITS4 primers (White et al., 1990) was carried out. The amplification reaction was performed with BIORAD thermocycler with the following protocol: incubation at 95°C for 3 min, 35 cycles at 95°C for 30 sec, 54°C for 30 sec, and 72 °C for 45 sec, followed by extension at 72°C for 7 min. The resulting ITS amplicon was purified with The Wizard® SV Gel and PCR Clean-Up System (Promega, Madison, WI, USA) and sent to the Sequencing Service of the Ludwig-Maximilians-Universität (LMU) in Munich (Germany) for sequencing. The ITS sequence was analyzed by BLASTn and identity of MUT 4178 isolate as *Tulasnella calospora* was confirmed.

Symbiotic and asymbiotic seed germination of Serapias vomeracea

Serapias vomeracea (BURM.) BRIQ. seeds were obtained from mature capsules collected from plants grown in the locality of Cairo Montenotte (SV) during spring 2019. To obtain symbiotic protocorms, the mycelium of the mycorrhizal fungus *T. calospora* (MUT 4178 isolate) and *S. vomeracea* seeds were co-inoculated in 9 cm Petri dishes as described in Perotto et al. (2014). Briefly, orchid seeds were surface sterilized in a solution of 1% sodium hypochlorite and 0.1% Tween-20 for 20 min under shaking, followed by three 5-minute rinses in sterile distilled water to remove residues of the sterilization solution. Seeds were re-suspended in sterile water and dropped on autoclaved cellulose membrane positioned on solid OA medium (0.3% oat flour, 1% agar) in 9 cm Petri dishes. In the center of each Petri dish, a plug (6 mm diameter) of actively growing *T. calospora* mycelium was placed, and plates were incubated at 23°C in full darkness for 45 days.

Asymbiotic protocorms were obtained by directly placing surface-sterilized *S. vomeracea* seeds on modified BM1 culture medium (Van Waes & Debergh, 1986) at 23°C in darkness for 90 days (Fochi, Chitarra, et al., 2017), with pH adjusted to 5.8. The fungal mycelium grown on the cellulose membrane next to the protocorms (MYC sample), symbiotic and asymbiotic protocorms were collected, immediately frozen in liquid nitrogen, and stored at −80°C for RNA extraction.

Gene identification and primer design

Identification of fungal genes coding for proteins putatively involved in sulfur (S) uptake, transfer and assimilation was performed using the *T. calospora* genome database on the Joint Genome Institute (JGI) fungal genome portal MycoCosm (http://genome.jgi.doe.gov/Tulca1/Tulca1.home.htm).

Selection of plant sequences coding for proteins potentially involved in S uptake, transfer and assimilation was performed using the RNA-Seq database obtained in the study of Fochi, Chitarra, et al. (2017) and a cDNA library obtained with a 454 GS-FLX Titanium pyrosequencing described in Perotto et al. (2014). Phylogenetic analysis of protein sequences putatively encoding for S transporters was performed through MEGAX software v. 11 including 62 sequences retrieved in NCBI Protein database and described as plant sulfate transporters (Table S1). A tree was generated using maximum likelihood (ML) method, by setting JTT model as substitution model and 500 bootstrap iterations.

PRIMER3PLUS (http://www.bioinformatics.nl/cgi-bin/primer3plus/primer3plus.cgi) was used to design specific primers for fungal and plant genes involved in S uptake and metabolism and their specificity was tested *in silico* using the tool PRIMER BLAST (https://www.ncbi.nlm.nih.gov/tools/primer-blast/) and through PCR experiments on DNA extracted from and *T. calospora* mycelium and *S. vomeracea* symbiotic protocorms.

RNA extraction and RT-qPCR

RNA extraction for RT-qPCR was conducted following the method of Chang et al. (1993) from symbiotic (SYMB) and asymbiotic (ASYMB) *S. vomeracea* protocorms as well as from *T. calospora* free-living mycelium (FLM) and mycelium grown on the cellulose membrane next to the mycorrhizal protocorms (MYC).

Before RNA quantification using the NanoDrop 1000, Turbo DNA-free TM reagent (Ambion, Austin, TX, USA) was used to remove genomic DNA according to the manufacturer's instructions. Absence of genomic DNA was checked through One-Step RT-PCR kit (Qiagen) using primers specific for fungal and plant housekeeping genes (see Table S2 and S3). cDNA synthesis was obtained using the SuperScriptII Reverse Transcriptase (Invitrogen, Thermo Fisher Scientific, Waltham, MA, USA), starting from approximately 500 ng of total RNA for each sample, following the manufacturer's instructions. At the end of the reaction, cDNA was diluted 1:10 for quantitative gene expression analysis, performed using a Rotor-Gene Q (Qiagen) instrument. Reactions were carried out in a final volume of 15 μl with 7.5 μl of Rotor-Gene SYBR® Green Master Mix, 5.5 μl of a mix of forward and reverse primers (prepared by adding 16 μl of each primer at 10 μM stock concentration to 168 μl of water) and 2 μl of cDNA. The RT-qPCR cycling program consisted of a 10 min/55°C RT step, 10 min/95°C holding step followed by 40 cycles of two steps (15 sec/95°C and 1 min/60°C).

Expression of target transcripts was quantified after normalization to the reference genes, that is, the fungal and plant elongation factor (EF) genes *TcEF-1α* and *SvEF-1α*, respectively, using the $2^{-\Delta\Delta CT}$ method (Livak & Schmittgen, 2001). Gene expression data were calculated as expression ratios. All reactions were performed with three biological and two technical replicates.

Laser microdissection and RT-PCR

To prepare tissue sections for laser microdissection (LMD), symbiotic protocorms were treated with Farmer's fixative (absolute ethanol/glacial acetic acid 3:1) and maintained at 4°C overnight; samples were successively dehydrated and embedded in paraffin as described in Fochi, Falla, et al., 2017, 12-μm thick sections were prepared using a rotational microtome and placed on Leica RNase-free PEN foil slides (Leica Microsystems) with ddH_2O filtered with a 0.2 μm filter. Slides were dried on a 40°C warming plate, stored at 4°C and used within 1 day. Before LMD cutting, the slides with the sections were submerged in Neoclear for 8–10 min, rinsed in 100% ethanol for 1 min, and then air-dried. A Leica LMD 6500 LMD system (Leica Microsystems, Inc., Germany) was used, in which the slides without paraffin were placed face-down on the microscope and cells containing visible fungal coils and uncolonized cells were collected in 0.5 ml tubes. Three biological replicates were prepared, in each of which approximately 1200–1300 cells were pooled. Every pool was eluted to a final volume of 50 μl with Pico Pure extraction buffer and RNA was extracted with Pico Pure kit (Life Technologies, Carlsbad, CA, USA) following the protocol with some modifications (*i.e.*, DNAse treatment was not done ion column). RNA was treated with Turbo DNA free (Ambion, Austin, TX, USA), according to the manufacturer's instructions.

RT-PCR reactions were carried out using the One-Step RT-PCR kit (Qiagen) in a final volume of 10 μl containing 2 μl of 5× buffer, 0.5 μl of 10 mM dNTPs, 0.25 μl of each primer (10 mM),

0.25 μl of One-Step RT-PCR enzyme mix and 0.5 μl of total RNA diluted 1:2. Samples were incubated for 30 min at 50°C, followed by 15 min at 95°C. After this step, amplification reactions were run for 40 cycles at 94°C for 30 sec, 60°C for 30 sec, and 72°C for 40 sec using the same *T. calospora* and *S. vomeracea* specific primers used for RT-qPCR (Table S2 and S3). DNA contamination in the RNA samples were checked using primers for the plant (*SvEF-1α*) and the fungal (*TcEF-1α*) housekeeping genes, following the One-Step RT-PCR protocol. PCR products were visualized after electrophoresis on a 1.5% agarose gel.

Statistical analysis

For statistical assessment of significant differences (*P*-value ≤0.05) in gene expression among conditions, REST© Relative expression software tool (Pfaffl et al., 2002) was used. The mathematical model used in this software is based on the correction for exact PCR efficiencies and the mean crossing point deviation between sample groups and control groups. Subsequently the expression ratio results of the investigated transcripts were tested for significance by a pairwise fixed reallocation randomization test ©.

Stable isotope tracer and high spatial resolution secondary ion mass spectrometry (SIMS)

Sample preparation and labeling

Seeds of *S. vomeracea* were surface sterilized in a solution of a sodium hypochlorite (0.5% available hypochlorite) for 1 min followed by three 1-minute rinses in sterile distilled water and germinated symbiotically on 0.3% OA medium with the fungus *T. calospora* for 1 month. The stable isotope tracers were provided to the fungal hyphae by using the same setup described by Kuga et al. (2014). Briefly, six symbiotically grown protocorms were transferred on an OA medium disc (5 mm in diameter) placed on the cap of a 0.5-ml Eppendorf tube overlying OA medium on a glass slide and kept in a moist Petri dish. 40 days after transfer, the fungal hyphae had reached the OA medium layer on the glass slide and 40 μl of an aqueous mixture of D-glucose (U-$^{13}C_6$, 99%; Cambridge Isotope Laboratories Inc., Andover, MA, USA), $^{15}NH_4{}^{15}NO_3$ (98%; Cambridge Isotope Laboratories Inc.), and $Mg^{34}SO_4$ (98%, Shoko science Co., Ltd., Yokohama, Kanagawa, Japan), at final concentrations of 1, 0.2, and 0.1%, respectively, were added to the OA medium below the plastic cap, so that only the hyphae that had reached it could absorb the tracers. All incubation processes and labeling of the symbiotic protocorms were conducted in the dark at 25°C. 6 days after the isotope tracers had been added to the hyphae, protocorms were fixed with 2.5% glutaraldehyde and 2% paraformaldehyde in 50 mM PIPES buffer (piperazine-1,4-bis (2-ethanesulfonic acid), pH 6.9) for 4 h at room temperature, cut in half with a sharp razor blade, and then post-fixed with 1% OsO_4 in the buffer for 2 h at room temperature. The fixed materials were then dehydrated with a graded ethanol series (50, 70, 80, 90, 95, and 100%). After infiltration with propylene oxide (50% and then 100%), samples were infiltrated and embedded in an epoxy resin (Embed-ltTM; Polysciences Inc., Warrington, PA, USA), which was polymerized at 70°C for 5 days. Semithin longitudinal sections were cut using glass knives and stained with toluidine blue O (TBO) to obtain structural information by light microscopy.

Isotope imaging of ^{34}S - ^{13}C- ^{15}N-labeled protocorms by isotope microscopy

For isotope measurements, 1 μm-thick sections were cut, transferred on a drop of distilled water placed on a silicon (Si) wafer (7 × 7 mm^2) put on a glass slide. The glass slide was placed on a hot plate so that the resin sections were adhered to the surface of the Si wafer, as described by Kuga et al. (2014). The sections on Si wafers were coated with a 70-nm layer of gold to prevent the accumulation of positive charge generated by the primary beam of the isotope microscope. The Hokudai isotope microscope system (Cameca IMS 1270 equipped with a stacked CMOS active pixel sensor, SCAPS) was used to visualize isotope distribution in cells, a technique known as isotopography (Hamasaki et al., 2013; Kuga et al., 2014; Takeda et al., 2019; Sakamoto et al., 2007; Yurimoto et al., 2003). A Cs^+ primary beam of 20 keV was homogeneously irradiated on the sample surface of c. 100 × 100 μm^2 was homogeneously irradiated with a Cs^+ primary beam of 20 keV and a beam current of c. 0.8 nA. Secondary ion images of $^{12}C^{14}N^-$, $^{12}C^{15}N^-$, $^{12}C^-$, $^{13}C^-$, $^{32}S^-$, and $^{34}S^-$ spattered from the sample surface were separated with a large-radius magnetic prism and transferred onto the SCAPS ion imager using stigmatic ion optics. Exposure times for each isotopograph were 10, 100, 10, 100, 50, and 150 sec, respectively. The exit slit was narrowed to prevent $^{13}C^{13}C^-$ and $^{10}B^{16}O^-$ from interfering with $^{12}C^{14}N^-$.

Region of interest (ROI) analysis

ImageJ (Fiji, 1.53 t; http://rsbweb.nih.gov/ij/) was used for the primary image processing and analyses. A set of the isotope images taken from one image site were aligned and made a ratio image as follows, for example, two of the ^{12}C images were processed to make one averaged image, and then $^{13}C/^{12}C$ ratio images were obtained by dividing the ^{13}C image by the averaged ^{12}C image (abbreviated as r13C in this study). $^{12}C^{15}N/^{12}C14N$ (abbreviated as r15N) and $^{34}S/^{32}S$ (abbreviated as r34S) images were produced similarly. 30 colonized cortical cells and 8 uncolonized cortical and meristematic cells were subjected to the region of interest (ROI) analysis. Using $^{12}C^{14}N$ and a light microscope TBO image, outlines of fungal peloton and host nucleus were defined using a polygonal selection tool.

Within the exact ROI of correlated r13C, r15N, and r34S images, the mean intensity, the standard deviation (SD), and the number of pixels (area) were obtained. The natural abundance of ^{13}C is 1.10% (limestone from a fossil belemnite), with an expected r13C value of 0.0111. The natural abundance of ^{15}N is 0.366% (N_2 gas in the atmosphere), with an expected rC15N value of 0.00367. The natural abundance of ^{34}S is 4.21% (the Vienna-Canyon Diablo Troilite), with an expected r32S value of 0.0437. Therefore, in this study, the values of r13C, rC15N, and r32S were multiplied by 100, 1000, and 100, respectively, so that the tracer isotope presences were detected if the analyzed values were larger than those of the natural abundances: 1.10, 3.67, and 4.37, respectively.

The comparisons between host nuclei of colonized and uncolonized cells of two protocorm regions were conducted by Tukey–Kramer test and correlations between hyphae and nuclei within colonized cells and between isotope ratios were analyzed by Pearson's correlation coefficient.

CONFLICT OF INTEREST STATEMENT

The authors declare no conflict of interest.

DATA AVAILABILITY STATEMENT

All relevant data can be found within the manuscript and its supporting materials.

ACKNOWLEDGMENTS

We thank Samuele Voyron and Stefania Daghino for supporting SDR during fungal isolate selection and growth. We also thank the anonymous reviewers for helpful comments on the manuscript. SDR was supported with a PhD fellowship by the Italian MUR.

SUPPORTING INFORMATION

Additional Supporting Information may be found in the online version of this article.

Table S1. Accession numbers of protein sequences retrieved from NCBI Protein database and described as plant S transporters used to generate phylogenetic tree of *Serapias vomeracea* protein sequences putatively encoding for S transporters (Figure 6).

Table S2. List of primers to amplify the *Tulasnella calospora* genes

Table S3. List of primers to amplify the *Serapias vomeracea* genes

Table S4. Fold change, standard error values and p-values of statistical assessment of differences performed by Relative Expression Software Tool REST© 2009 v. 2.0.13 of *T. calospora* genes in MYC and SYMB conditions compared to FLM.

Table S5. Fold change, standard error values and p-values of statistical assessment of differences performed by Relative Expression Software Tool REST© 2009 v. 2.0.13 of *S. vomeracea* genes in symbiotic conditions compared to asymbiotic.

REFERENCES

Allen, J.W. & **Shachar-Hill, Y.** (2009) Sulfur transfer through an arbuscular mycorrhiza. *Plant Physiology*, **149**, 549–560.

Balestrini, R., **Berta, G.** & **Bonfante, P.** (1992) The plant nucleus in mycorrhizal roots: positional and structural modifications. *Biology of the Cell*, **75**, 235–243.

Balestrini, R. & **Bonfante, P.** (2005) The interface compartment in arbuscular mycorrhizae: a special type of plant cell wall? *Plant Biosystems*, **139**, 8–15.

Balestrini, R. & **Bonfante, P.** (2014) Cell wall remodeling in mycorrhizal symbiosis: a way towards biotrophism. *Frontiers in Plant Science*, **5**, 237.

Balestrini, R. & **Lumini, E.** (2018) Focus on mycorrhizal symbioses. *Applied Soil Ecology*, **123**, 299–304.

Baron, N.C. & **Rigobelo, E.C.** (2022) Endophytic fungi: a tool for plant growth promotion and sustainable agriculture. *Mycology*, **13**, 39–55.

Bohman, B., **Phillips, R.D.**, **Flematti, G.R.**, **Barrow, R.A.** & **Peakall, R.** (2017) The spider orchid *Caladenia crebra* produces sulfurous pheromone mimics to attract its male wasp pollinator. *Angewandte Chemie International Edition*, **56**, 8455–8458.

Bucher, M., **Hause, B.**, **Krajinski, F.** & **Küster, H.** (2014) Through the doors of perception to function in arbuscular mycorrhizal symbioses. *New Phytologist*, **204**, 833–840.

Cagnac, O., **Bourbouloux, A.**, **Chakrabarty, D.**, **Zhang, M.Y.** & **Delrot, S.** (2004) AtOPT6 transports glutathione derivatives and is induced by primisulfuron. *Plant Physiology*, **135**, 1378–1387.

Cameron, D.D., **Leake, J.R.** & **Read, D.J.** (2006) Mutualistic mycorrhiza in orchids: evidence from plant–fungus carbon and nitrogen transfers in the green-leaved terrestrial orchid *Goodyera repens*. *New Phytologist*, **171**, 405–416.

Cao, M.J., **Wang, Z.**, **Wirtz, M.**, **Hell, R.**, **Oliver, D.J.** & **Xiang, C.B.** (2013) SULTR 3; 1 is a chloroplast-localized sulfate transporter in Arabidopsis thaliana. *The Plant Journal*, **73**, 607–616.

Card, S., **Johnson, L.**, **Teasdale, S.** & **Caradus, J.** (2016) Deciphering endophyte behaviour: the link between endophyte biology and efficacious biological control agents. *FEMS Microbiology Ecology*, **92**, fiw114.

Casieri, L., **Ait Lahmidi, N.**, **Doidy, J.**, **Veneault-Fourrey, C.**, **Couturier-Migeon, A.**, **Bonneau, L.** ***et al.*** (2013) Biotrophic transportome in mutualistic plant-fungal interactions. *Mycorrhiza*, **23**, 597–625.

Casieri, L., **Gallardo, K.** & **Wipf, D.** (2012) Transcriptional response of *Medicago truncatula* sulphate transporters to arbuscular mycorrhizal symbiosis with and without sulphur stress. *Planta*, **235**, 1431–1447.

Chan, K.X., **Phua, S.Y.** & **Van Breusegem, F.** (2019) Secondary sulfur metabolism in cellular signalling and oxidative stress responses. *Journal of Experimental Botany*, **70**, 4237–4250.

Chang, S., **Puryear, J.** & **Carney, J.** (1993) A simple and efficient method for isolating RNA from pine trees. *Plant Molecular Biology Reporter*, **11**, 113–116.

Chen, Z., **Zhao, P.X.**, **Miao, Z.Q.**, **Qi, G.F.**, **Wang, Z.**, **Yuan, Y.** ***et al.*** (2019) SULTR3s function in chloroplast sulfate uptake and affect ABA biosynthesis and the stress response. *Plant Physiology*, **180**, 593–604.

Dearnaley, J.D.W. & **Cameron, D.D.** (2017) Nitrogen transport in the orchid mycorrhizal symbiosis – further evidence for a mutualistic association. *New Phytologist*, **213**, 10–12.

Deslandes, L. & **Rivas, S.** (2011) The plant cell nucleus: a true arena for the fight between plants and pathogens. *Plant Signaling & Behavior*, **6**, 42–48.

Fochi, V., **Chitarra, W.**, **Kohler, A.**, **Voyron, S.**, **Singan, V.R.**, **Lindquist, E.A.** ***et al.*** (2017) Fungal and plant gene expression in the *Tulasnella calospora–Serapias vomeracea* symbiosis provides clues about N pathways in orchid mycorrhizas. *New Phytologist*, **213**, 365–379.

Fochi, V., **Falla, N.**, **Girlanda, M.**, **Perotto, S.** & **Balestrini, R.** (2017) Cell-specific expression of plant nutrient transporter genes in orchid mycorrhizae. *Plant Science*, **263**, 39–45.

Gebauer, G., **Preiss, K.** & **Gebauer, A.C.** (2016) Partial mycoheterotrophy is more widespread among orchids than previously assumed. *New Phytologist*, **211**, 11–15.

Genre, A., **Lanfranco, L.**, **Perotto, S.** & **Bonfante, P.** (2020) Unique and common traits in mycorrhizal symbioses. *Nature Reviews Microbiology*, **18**, 649–660.

Gigolashvili, T. & **Kopriva, S.** (2014) Transporters in plant sulfur metabolism. *Frontiers in Plant Science*, **5**, 442.

Giovannetti, M., **Tolosano, M.**, **Volpe, V.**, **Kopriva, S.** & **Bonfante, P.** (2014) Identification and functional characterization of a sulfate transporter induced by both sulfur starvation and mycorrhiza formation in *Lotus japonicus*. *New Phytologist*, **204**, 609–619.

Girlanda, M., **Segreto, R.**, **Cafasso, D.**, **Liebel, H.T.**, **Rodda, M.**, **Ercole, E.** ***et al.*** (2011) Photosynthetic Mediterranean meadow orchids feature partial mycoheterotrophy and specific mycorrhizal associations. *American Journal of Botany*, **98**, 1148–1163.

Hamasaki, T., **Matsumoto, T.**, **Sakamoto, N.**, **Shimahara, A.**, **Kato, S.**, **Yoshitake, A.** ***et al.*** (2013) Synthesis of 18O-labeled RNA for application to kinetic studies and imaging. *Nucleic Acids Research*, **41**, e126.

Hell, R. (1997) Molecular physiology of plant sulfur metabolism. *Planta*, **202**, 138–148.

Hynson, N.A., **Madsen, T.P.**, **Selosse, M.A.**, **Adam, I.K.U.**, **Ogura-Tsujita, Y.**, **Roy, M.** ***et al.*** (2013) The physiological ecology of mycoheterotrophic plants. In: Merckx, V.S.F.T. (Ed.) *Mycoheterotrophy: the biology of plants living on fungi*. New York: Springer, pp. 297–342.

Ivanov, S., **Austin, J.**, **Berg, R.H.** & **Harrison, M.J.** (2019) Extensive membrane systems at the host–arbuscular mycorrhizal fungus interface. *Nature Plants*, **5**, 194–203.

Kataoka, T., **Hayashi, N.**, **Yamaya, T.** & **Takahashi, H.** (2004) Root-to-shoot transport of sulfate in *Arabidopsis*. Evidence for the role of SULTR3;5 as a component of low-affinity sulfate transport system in the root vasculature. *Plant Physiology*, **136**, 4198–4204.

Kaur, J. & **Bachhawat, A.K.** (2007) Yct1p, a novel, high-affinity, cysteine-specific transporter from the yeast *Saccharomyces cerevisiae*. *Genetics*, **176**, 877–890.

Kohler, A., **Kuo, A.**, **Nagy, L.G.**, **Morin, E.**, **Barry, K.W.**, **Buscot, F.** ***et al.*** (2015) Convergent losses of decay mechanisms and rapid turnover of symbiosis genes in mycorrhizal mutualists. *Nature Genetics*, **47**, 410–415.

Kopriva, S., **Malagoli, M.** & **Takahashi, H.** (2019) Sulfur nutrition: impacts on plant development, metabolism, and stress responses. *Journal of Experimental Botany*, **70**, 4069–4073.

Kopriva, S., **Mugford, S.G.**, **Baraniecka, P.**, **Lee, B.R.**, **Matthewman, C.A.** & **Koprivova, A.** (2012) Control of sulfur partitioning between primary and secondary metabolism in *Arabidopsis*. *Frontiers in Plant Science*, **3**, 163.

Kopriva, S., **Talukdar, D.**, **Takahashi, H.**, **Hell, R.**, **Sirko, A.**, **D'Souza, S.F.** ***et al.*** (2016) Frontiers of sulfur metabolism in plant growth, development, and stress response. *Frontiers in Plant Science*, **6**, 1220.

Kuga, Y., **Sakamoto, N.** & **Yurimoto, H.** (2014) Stable isotope cellular imaging reveals that both live and degenerating fungal pelotons transfer carbon and nitrogen to orchid protocorms. *New Phytologist*, **202**, 594–605.

Lee, C.P., **Wirtz, M.** & **Hell, R.** (2014) Evidence for several cysteine transport mechanisms in the mitochondrial membranes of *Arabidopsis thaliana*. *Plant and Cell Physiology*, **55**, 64–73.

Li, Q., **Gao, Y.** & **Yang, A.** (2020) Sulfur homeostasis in plants. *International Journal of Molecular Sciences*, **21**, 8926.

Liebel, H.T., **Bidartondo, M.I.**, **Preiss, K.**, **Segreto, R.**, **Stöckel, M.**, **Rodda, M.** ***et al.*** (2010) C and N stable isotope signatures reveal constraints to nutritional modes in orchids from the Mediterranean and Macaronesia. *American Journal of Botany*, **97**, 903–912.

Linder, T. (2018) Assimilation of alternative sulfur sources in fungi. *World Journal of Microbiology and Biotechnology*, **34**, 1–7.

Livak, K.J. & **Schmittgen, T.D.** (2001) Analysis of relative gene expression data using real-time quantitative PCR and the 2− ΔΔCT method. *Methods*, **25**, 402–408.

Ma, Q., **Chadwick, D.R.**, **Wu, L.** & **Jones, D.L.** (2022) Arbuscular mycorrhiza fungi colonisation stimulates uptake of inorganic nitrogen and Sulphur but reduces utilisation of organic forms in tomato. *Soil Biology and Biochemistry*, **172**, 108719.

Mansouri-Bauly, H., **Kruse, J.**, **Sýkorová, Z.**, **Scheerer, U.** & **Kopriva, S.** (2006) Sulfur uptake in the ectomycorrhizal fungus *Laccaria bicolor* S238N. *Mycorrhiza*, **16**, 421–427.

Miura, C., **Yamaguchi, K.**, **Miyahara, R.**, **Yamamoto, T.**, **Fuji, M.**, **Yagame, T.** ***et al.*** (2018) The mycoheterotrophic symbiosis between orchids and mycorrhizal fungi possesses major components shared with mutualistic plant-mycorrhizal symbioses. *Molecular Plant-Microbe Interactions*, **31**, 1032–1047.

Narayan, O.P., **Kumar, P.**, **Yadav, B.**, **Dua, M.** & **Johri, A.K.** (2022) Sulfur nutrition and its role in plant growth and development. *Plant Signaling & Behavior*. https://doi.org/10.1080/15592324.2022.2030082

Narayan, O.P., **Verma, N.**, **Jogawat, A.**, **Dua, M.** & **Johri, A.K.** (2021) Sulfur transfer from the endophytic fungus *Serendipita indica* improves maize growth and requires the sulfate transporter SiSulT. *The Plant Cell*, **33**, 1268–1285.

Oktalira, F.T., **May, T.W.**, **Dearnaley, J.D.W.** & **Linde, C.C.** (2021) Seven new *Serendipita* species associated with Australian terrestrial orchids. *Mycologia*, **113**, 968–987.

Perotto, S., **Rodda, M.**, **Benetti, A.**, **Sillo, F.**, **Ercole, E.**, **Rodda, M.** ***et al.*** (2014) Gene expression in mycorrhizal orchid protocorms suggests a friendly plant–fungus relationship. *Planta*, **239**, 1337–1349.

Pfaffl, M.W., **Horgan, G.W.** & **Dempfle, L.** (2002) Relative expression software tool (REST©) for group-wise comparison and statistical analysis of relative expression results in real-time PCR. *Nucleic Acids Research*, **30**, 36.

Piłsyk, S. & **Paszewski, A.** (2009) Sulfate permease sphylogenetic diversity of sulfate transport. *Acta Biochimica Polonica*, **56**, 3.

Ristova, D. & **Kopriva, S.** (2022) Sulfur signaling and starvation response in *Arabidopsis*. *Iscience*, **25**, 104242.

Sacchi, G.A. & **Nocito, F.F.** (2019) Plant sulfate transporters in the low phytic acid network: some educated guesses. *Plants*, **8**, 616.

Sakamoto, N., **Seto, Y.**, **Itoh, S.**, **Kuramoto, K.**, **Fujino, K.**, **Nagashima, K.**, **Krot, A.N.** & **Yurimoto, H.** (2007) Remnants of the early solar system water enriched in heavy oxygen isotopes. *Science*, **317**, 231–233.

Schiebold, J.M.-I., **Bidartondo, M.I.**, **Lenhard, F.**, **Makiola, A.** & **Gebauer, G.** (2017) Exploiting mycorrhizas in broad daylight: partial mycoheterotrophy is a common nutritional strategy in meadow orchids M. Heijden, ed. *Journal of Ecology*, **106**, 168–178.

Schumann, U., **Smith, N.A.** & **Wang, M.B.** (2013) A fast and efficient method for preparation of high-quality RNA from fungal mycelia. *BMC Research Notes*, **6**, 71.

Sieh, D., **Watanabe, M.**, **Devers, E.A.**, **Brueckner, F.**, **Hoefgen, R.** & **Krajinski, F.** (2013) The arbuscular mycorrhizal symbiosis influences sulfur starvation responses of *Medicago truncatula*. *New Phytologist*, **197**, 606–616.

Smith, S.E. & **Read, D.J.** (2008) *Mycorrhizal Symbiosis*, 3rd edition. London: Academic Press.

Stöckel, M., **Těšitelová, T.**, **Jersáková, J.**, **Bidartondo, M.I.** & **Gebauer, G.** (2014) Carbon and nitrogen gain during the growth of orchid seedlings in nature. *New Phytologist*, **202**, 606–615.

Takahashi, H. (2019) Sulfate transport systems in plants: functional diversity and molecular mechanisms underlying regulatory coordination. *Journal of Experimental Botany*, **70**, 4075–4087.

Takahashi, H., **Kopriva, S.**, **Giordano, M.**, **Saito, K.** & **Hell, R.** (2011) Sulfur assimilation in photosynthetic organisms: molecular functions and regulations of transporters and assimilatory enzymes. *Annual Review of Plant Biology*, **62**, 157–184.

Takahashi, H., **Watanabe-Takahashi, A.**, **Smith, F.W.**, **Blake-Kalff, M.**, **Hawkesford, M.J.** & **Saito, K.** (2000) The roles of three functional sulphate transporters involved in uptake and translocation of sulphate in *Arabidopsis thaliana*. *The Plant Journal*, **23**, 171–182.

Takeda, T., **Doiyama, S.**, **Azumi, J.**, **Shimada, Y.**, **Tokuji, Y.**, **Yamaguchi, H.** ***et al.*** (2019) Organogermanium suppresses cell death due to oxidative stress in normal human dermal fibroblasts. *Scientific Reports*, **9**, 13637.

Traynor, A.M., **Sheridan, K.J.**, **Jones, G.W.**, **Calera, J.A.** & **Doyle, S.** (2019) Involvement of sulfur in the biosynthesis of essential metabolites in pathogenic fungi of animals, particularly *Aspergillus* spp.: molecular and therapeutic implications. *Frontiers in Microbiology*, **10**, 2859.

Uetake, Y., **Kobayashi, K.** & **Ogoshi, A.** (1992) Ultrastructural changes during the symbiotic development of *Spiranthes sinensis* (Orchidaceae) protocorms associated with binucleate *Rhizoctonia* anastomosis group C. *Mycological Research*, **96**, 199–209.

Valadares, R.B.S., **Marroni, F.**, **Sillo, F.**, **Oliveira, R.R.M.**, **Balestrini, R.** & **Perotto, S.** (2021) A transcriptomic approach provides insights on the mycorrhizal symbiosis of the Mediterranean orchid *Limodorum abortivum* in nature. *Plants*, **10**, 251–268.

Valadares, R.B.S., **Perotto, S.**, **Lucheta, A.R.**, **Santos, E.C.**, **Oliveira, R.M.** & **Lambais, M.R.** (2020) Proteomic and transcriptomic analyses indicate metabolic changes and reduced defense responses in mycorrhizal roots of *Oeceoclades maculata* (Orchidaceae) collected in nature. *Journal of Fungi*, **6**, 148–168.

Van Waes, J.M. & **Debergh, P.C.** (1986) *In vitro* germination of some Western European orchids. *Physiologia Plantarum*, **67**, 253–261.

White, T.J., **Bruns, T.**, **Lee, S.** & **Taylor, J.W.** (1990) Amplification and direct sequencing of fungal ribosomal RNA genes for phylogenetics. In: Innis, M.A., Gelfand, D.H., Sninsky, J.J. & White, T.J. (Eds.) *PCR protocols: a guide to methods and applications*. New York, NY, USA: Academic Press, pp. 315–322.

Wu, S., **Hu, Y.**, **Zhang, X.**, **Sun, Y.**, **Wu, Z.**, **Li, T.**, **Lv, J.**, **Li, J.**, **Zhang, J.**, **Zheng, L.**, **Huang, L.** & **Chen, B.** (2018) Chromium detoxification in arbuscular mycorrhizal symbiosis mediated by sulfur uptake and metabolism. *Environmental and Experimental Botany*, **147**, 43–52.

Yang, G., **Wei, Q.**, **Huang, H.** & **Xia, J.** (2020) Amino acid transporters in plant cells: a brief review. *Plants*, **9**, 967.

Yurimoto, H., **Nagashima, K.** & **Kunihiro, T.** (2003) High precision isotope micro-imaging of materials. *Applied Surface Science*, **203**, 793–797.

Zenda, T., **Liu, S.**, **Dong, A.** & **Duan, H.** (2021) Revisiting Sulphur—the once neglected nutrient: It's roles in plant growth, metabolism, stress tolerance and crop production. *Agriculture*, **11**, 626.

Zhang, Z., **Xie, Q.**, **Jobe, T.O.**, **Kau, A.R.**, **Wang, C.**, **Li, Y.** ***et al.*** (2016) Identification of AtOPT4 as a plant glutathione transporter. *Molecular Plant*, **9**, 481–484.

Zhao, H., **Frank, T.**, **Tan, Y.**, **Zhou, C.**, **Jabnoune, M.**, **Arpat, A.B.** ***et al.*** (2016) Disruption of OsSULTR3;3 reduces phytate and phosphorus concentrations and alters the metabolite profile in rice grains. *New Phytologist*, **211**, 926–939.

Zheng, Z.L., **Zhang, B.** & **Leustek, T.** (2014) Transceptors at the boundary of nutrient transporters and receptors: a new role for *Arabidopsis* SULTR1; 2 in sulfur sensing. *Frontiers in Plant Science*, **5**, 710.

Zuber, H., **Davidian, J.C.**, **Aubert, G.**, **Aimé, D.**, **Belghazi, M.**, **Lugan, R.** ***et al.*** (2010) The seed composition of *Arabidopsis* mutants for the group 3 sulfate transporters indicates a role in sulfate translocation within developing seeds. *Plant Physiology*, **154**, 913–926.